# On the kinetic barriers of graphene homo-epitaxy

Wei Zhang, Xinke Yu, Erica Cahyadi, Ya-Hong Xie, and Christian Ratsch

Citation: Applied Physics Letters **105**, 221607 (2014); doi: 10.1063/1.4903485
View online: http://dx.doi.org/10.1063/1.4903485
View Table of Contents: http://scitation.aip.org/content/aip/journal/apl/105/22?ver=pdfcov
Published by the AIP Publishing

# On the kinetic barriers of graphene homo-epitaxy

Wei Zhang,[1] Xinke Yu,[1] Erica Cahyadi,[1,2] Ya-Hong Xie,[1,a)] and Christian Ratsch[3]
[1]*Department of Materials Science & Engineering, University of California Los Angeles, Los Angeles, California 90095, USA*
[2]*GLOBALFOUNDRIES Inc., Malta, New York 12020, USA*
[3]*Department of Mathematics and Institute for Pure and Applied Mathematics, University of California Los Angeles, Los Angeles, California 90095, USA*

(Received 15 October 2014; accepted 23 November 2014; published online 4 December 2014)

The diffusion processes and kinetic barriers of individual carbon adatoms and clusters on graphene surfaces are investigated to provide fundamental understanding of the physics governing epitaxial growth of multilayer graphene. It is found that individual carbon adatoms form bonds with the underlying graphene whereas the interaction between graphene and carbon clusters, consisting of 6 atoms or more, is very weak being van der Waals in nature. Therefore, small carbon clusters are quite mobile on the graphene surfaces and the diffusion barrier is negligibly small (~6 meV). This suggests the feasibility of high-quality graphene epitaxial growth at very low growth temperatures with small carbon clusters (e.g., hexagons) as carbon source. We propose that the growth mode is totally different from 3-dimensional bulk materials with the surface mobility of carbon hexagons being the highest over graphene surfaces that gradually decreases with further increase in cluster size. © *2014 AIP Publishing LLC*. [http://dx.doi.org/10.1063/1.4903485]

Graphene has attracted intensive attention in the past decade due to its unique electrical, thermal, and mechanical properties.[1–3] Multilayer graphene (MLG) consisting of two or more layers of graphene is also of interest for various applications including transparent electrodes for organic devices,[4,5] solar cells,[6] field-effect transistors,[7] field emission displays,[8] photo-detectors,[9] and highly efficient thermal interface materials.[10] The crux of MLG fabrication is the growth dynamics of graphene homo-epitaxy. This dynamic process is expected to be fundamentally different between 2-dimensional materials (also known as van der Waals materials) and their 3-dimensional counterparts for which there exists an extensive knowledge base. Different techniques have been used to fabricate MLG including low-temperature chemical vapor deposition on Ni catalyst,[6] microwave plasma enhanced chemical vapor deposition,[8,11] and transferring and stacking large-area CVD-grown graphene monolayers.[12] To date, no proven approach allows for precise control of the number of layers presumably due to the lack of fundamental understanding of the dynamics of epitaxy. In this work, we report the results of an *ab initio* study of various plausible modes of graphene epitaxy over graphene surfaces using density-functional theory (DFT).

Our calculations are based on DFT as implemented in the Fritz Haber Institute *ab initio* molecular simulations package (FHI-AIMS).[13] This is an all-electron full potential DFT code that uses numeric atom centered orbitals as its basis set. We have used the parameters as they are implemented in FHI-AIMS in the default setting "light" which has radial s, p, and d characters with an overall cutoff radius of 5 Å and a Hartree potential expansion up to $l = 4$. The accuracy of the total energy is tested to be within 0.01 eV compared with that obtained using the default setting "tight" (overall cutoff radius of 6 Å and $l = 6$).[13] We use the Perdew-Burke-Ernzerhof (PBE) approximation of the generalized gradient approximation (GGA) for the exchange-correlation functional.[14] It is a well-known problem that inter-layer graphitic bonding due to van der Waals (vdW) forces is not properly described within the standard DFT framework. This is most dramatic for graphite where the DFT-GGA results yield a slight repulsion of around 10–20 meV per atom between individual carbon sheets. We therefore use the Tkatchenko-Scheffler method[15] to include vdW interactions in the DFT calculations. The graphene lattice constant is calculated to be 2.465 Å in good agreement with previous results.[16] To model the diffusion of carbon atoms or clusters on monolayer graphene, we use a 17.25 Å × 17.08 Å graphene supercell (7-hexagon wide in the x-direction and 8-hexagon wide in the y-direction) comprising of 112 carbon atoms with a vacuum region of 50 Å in the z-direction. A $4 \times 4 \times 1$ k-point grid is used for the calculations. The convergence of the results has been carefully tested with respect to the system size, the basis set, and the density of the (numerical) integration mesh.

First, we investigate the diffusion of individual carbon adatoms on monolayer graphene. The preferred adsorption sites are the bridge sites about 1.89 Å above the graphene plane with an adsorption energy of −2.70 eV. It is shown as position A in Fig. 1(a). The absorption energy $\Delta E_a$ of a carbon adatom on monolayer graphene is defined as

$$\Delta E_a = E_{total} - E_g - E_c, \quad (1)$$

where $E_{total}$ is the total DFT energy of the carbon adatom-graphene system, and $E_g$ and $E_c$ are the total DFT energies of an isolated graphene monolayer and an isolated carbon atom, respectively. All of the energies mentioned above are negative in value. In order to diffuse across the graphene surface, a carbon adatom has to cross the transition site shown as position T in Fig. 1(a). The nudged elastic band method

a)Author to whom correspondence should be addressed. Electronic mail: yahong.xie@gmail.com

 

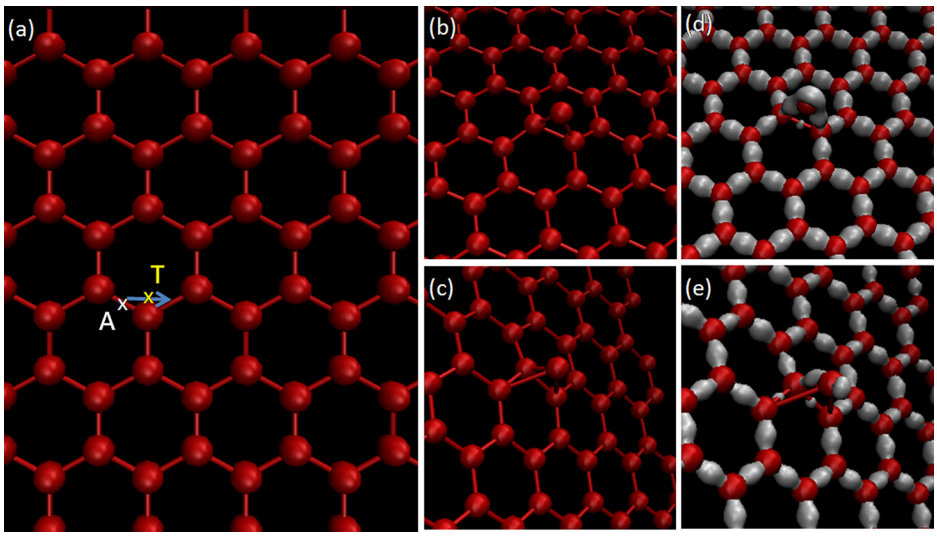


FIG. 1. (a) Adsorption site (A) and transition site (T) for a carbon adatom on graphene, (b) side view of adsorption site, (c) side view of transition site, and the corresponding electron density difference plots (d) and (e).

(NEB) is used to find the minimum energy path (MEP) and the transition site.[17,18] The diffusion barrier for an adatom to hop along the path indicated in Fig. 1(a) is about 0.48 eV. Figs. 1(b) and 1(c) show the side view of site A and T. The corresponding electron density difference plots are shown in Figs. 1(d) and 1(e). They are obtained by subtracting the electron densities of individual carbon atoms (no interaction among each other) sitting in the same positions as the adatom-graphene system from that of the adatom-graphene system. Therefore, they represent a net change of the electron densities from which the bonding information [white part in Figs. 1(d) and 1(e)] of the adatom-graphene system can be extracted. It can be seen from Fig. 1(d) at the adsorption site A that the carbon adatom forms covalent bonds with two neighboring atoms in the graphene layer underneath. This accounts for the strong interaction between the carbon adatom and the graphene layer, and thus the larger adsorption energy and diffusion barrier compared to other carbon clusters of bigger sizes diffusing on graphene. Details will be discussed in the following text.

We continue to study the diffusion of carbon dimers, trimers, tetramers, pentamers, and hexagons. For each cluster size, more than 10 plausible configurations have been tested to find the most preferred configuration and adsorption site. Trimers and pentamers behave in a similar fashion as dimers and tetramers within the accuracy of the calculation and are excluded here for brevity. Figs. 2(a)–2(c) show these configurations of the diffusing species at the adsorption sites and the bonding information obtained in the same way as discussed previously. The adsorption energies per carbon atom of dimers, tetramers and hexagons are −5.47 eV, −6.91 eV, and −7.27 eV, respectively. The absorption energy $\Delta E_a$ can be defined as

$$\Delta E_a = E_{total} - E_g - nE_c, \quad (2)$$

where $E_{total}$ is the total energy of the carbon cluster-graphene system, n is the number of carbon atoms in the cluster, and $E_g$ and $E_c$ are the total energies of an isolated graphene monolayer and an isolated carbon adatom, respectively. Since the adsorption energy per atom decreases as the size of cluster becomes bigger, it is energetically favorable for the carbon atoms to stick together and form clusters instead of standing alone as individual adatoms. As can be seen from Figs. 2(a)–2(c), dimers and tetramers prefer to sit upright at the bridge site about 1.88 Å and 1.81 Å above the graphene layer whereas hexagons prefer to lay flat floating about 3.25 Å above the graphene layer. Dimers and tetramers form covalent bonds with the neighboring two atoms of the graphene layer in a similar way as an individual carbon adatom. The diffusion barriers for dimers and tetramers are about 0.25 eV and 0.35 eV, respectively, both smaller than the barrier for an individual carbon adatom. On the other hand, there are no covalent bonds formed between hexagons and graphene and only vdW forces are present. The bonding energy between hexagons and graphene is quite small being about 80 meV per atom, which results in a very small diffusion barrier of about 6 meV. This means that compared to an individual carbon adatoms, dimers or tetramers, hexagons are much more mobile and may move more freely on the graphene surface. It is instructive to compare these diffusion barrier values to that of Si adatoms diffusing on Si(100) surfaces which is about 1 eV.[19] This suggests that all carbon species from monomers to other clusters diffusing on the graphene surfaces are much faster than Si adatoms on Si(001) surfaces. Therefore, we expect that during the homoepitaxy of graphene, the islands grown will be much larger and much further separated than in the case of Si on Si(001) at the same growth temperature.

At least 5 plausible configurations have been tested to find the most preferred configuration and adsorption sites for several cluster sizes larger than 6 carbon atoms. When the number of carbon atoms in the cluster is larger than 6, the clusters tend to form flat rings floating over graphene surface, as shown in Figs. 3(a) and 3(b). When the size of the cluster reaches 13 carbon atoms or more, a flat and compact graphene-like configuration can be formed above the graphene surface as shown in Figs. 3(c)–3(e). Like hexagons, no covalent bonds are formed between clusters and graphene with only vdW forces present. We plot the adsorption energies per atom for the clusters of different configurations as a function of number of atoms in Fig. 4. The adsorption energies per atom for flat ring configurations first drop sharply with increasing cluster size and reach a minimum at the size

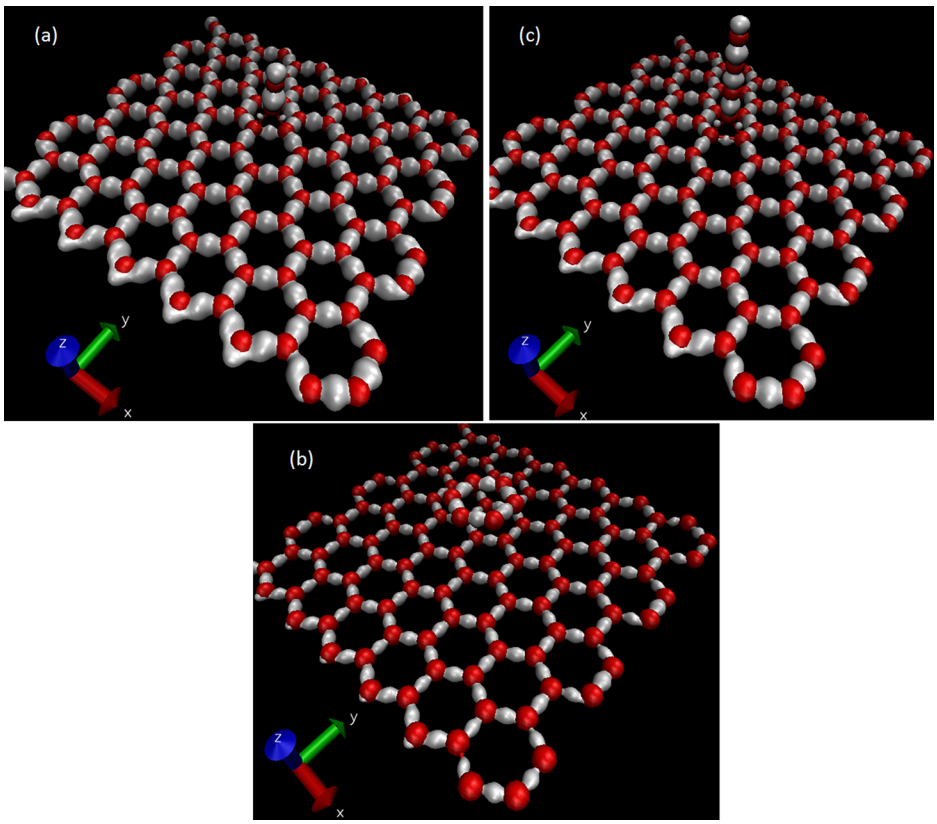


FIG. 2. The electron density difference plots showing the most preferred configurations with bonding information for (a) dimer, (b) tetramer, and (c) hexagon.

of about 54 carbon atoms. Then it goes up, presumably approaching −6.56 eV, which is the adsorption energy per atom for an infinite carbon atom string. The adsorption energy per atom for graphene-like configurations slowly approaches the binding energy per atom for a full graphene layer, which we have calculated as −9.23 eV per atom (in AB stacking). Compared to flat ring configurations, the compact graphene-like configuration is less energetically favored until the size of cluster increases to about 24 carbon atoms. However, we speculate that due to the kinetic limitations, clusters of size less than 24 carbon atoms might also form metastable graphene-like configurations. The kinetic pathway for the transition from flat ring configuration to graphene-like configurations is not yet known. When

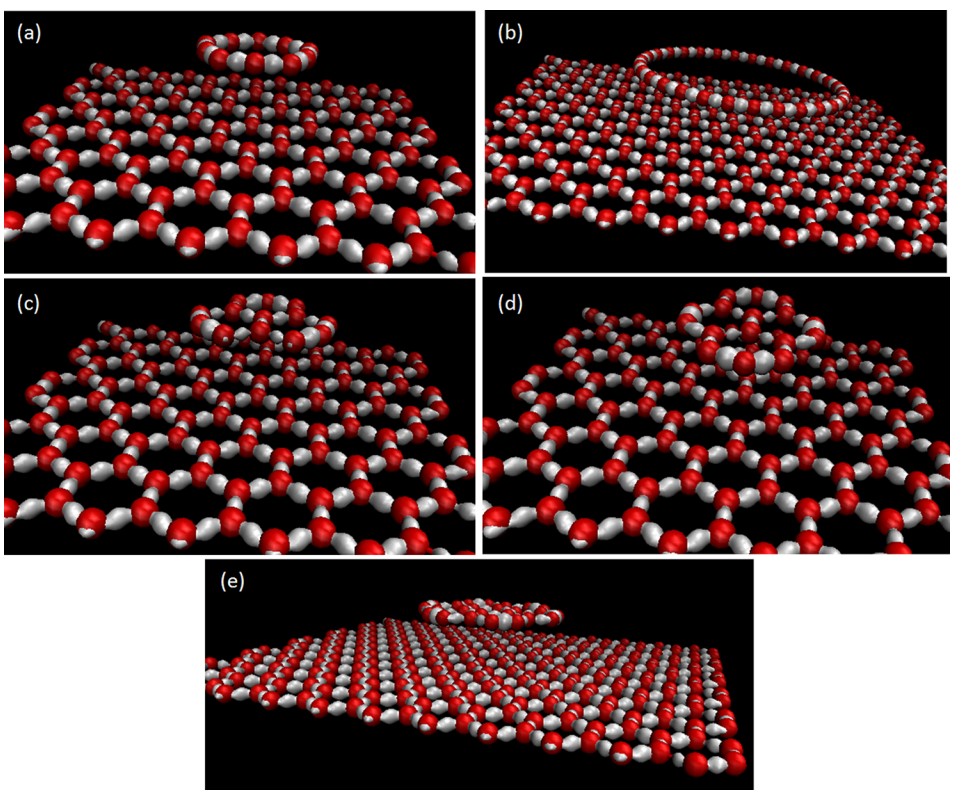


FIG. 3. Stable flat ring configurations for (a) 10 carbon atoms, and (b) 30 carbon atoms; stable compact graphene-like configurations for (c) 13 carbon atoms, (d) 16 carbon atoms, and (e) 24 carbon atoms.

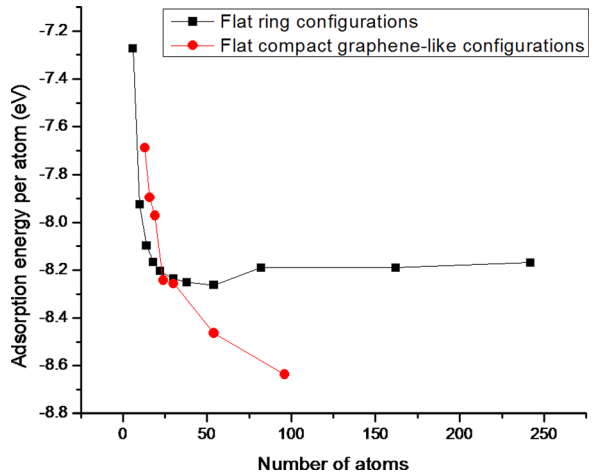


FIG. 4. Adsorption energies per atom as a function of number of atoms.

considering surface diffusion of carbon clusters, it is important to keep in mind the fundamental difference between islands/clusters of carbon over graphene surface and those of 3-dimensional crystals such as Si over Si surface. The former is more mobile than individual carbon adatoms whereas the latter is stationary for all practical purposes. By far, majority of the total adsorption energy of $\Delta E_a$ comes from the C–C bonds in the plane of the island/cluster. The strong C–C bonds within individual island/cluster imply their very low "2-dimensional vapor pressures." In other words, the carbon adatom density in the presence of graphene islands in equilibrium is expected to be orders of magnitude lower than that of Si adatoms in the presence of Si 2-dimensional islands at comparable temperatures. The surface diffusion barriers shown in Fig. 5 are typically less than 10% of $\Delta E_{a.}$ This is one of the unique characteristics of van der Waals materials. The surface diffusion barrier height increases nearly linearly with increasing cluster size. This is because each carbon atom in the cluster contributes to the total vdW force, which is the origin of the energy barrier. Therefore, the carbon

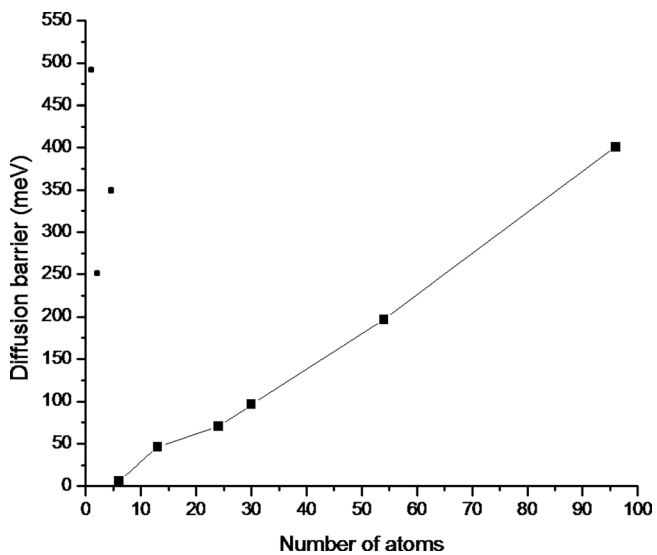


FIG. 5. Diffusion barriers for graphene-like clusters as a function of number of atoms. Also shown are the diffusion barriers for single carbon atoms, dimers, and tetramers.

clusters will eventually become immobile again with increasing size of the clusters. To put things in perspective, we know from Fig. 5 that the diffusion barrier of graphene islands/clusters on a graphene surface approaches that of individual Si adatoms on Si (001) surface only when the cluster size reaches about 200. This means that on pristine graphene surfaces, one would expect that epitaxial growth of a second layer of graphene can be carried out at much lower substrate temperatures than for 3-dimensional crystals.

Based on the calculation results presented above, we believe that the growth mode for graphene homoepitaxy is completely different from the established conventional growths modes for 3-dimensional bulk materials. For the epitaxy of 3-dimensional materials, single adatoms are typically the fastest moving entities on the surface. They collide and interact with one another to form clusters. When a critical size is reached stochastically, a cluster becomes thermodynamically stable and acts as a sink for additional adatoms in the island nucleation/coalescence mode of growths. Alternatively, adatoms diffuse along the surface until encountering an existing step edge where they incorporate in the step-flow growth mode. However, for epitaxial growths of vdW materials such as graphene on graphene, the process appears to be that monomers and small clusters are relatively stationary on the surface because of the covalent bonds they form with the underlying graphene, whereas clusters of size 6 or more diffuse freely on the graphene surface and incorporate smaller clusters and adatoms along the way. The process continues with these large clusters experiencing growth in size while losing mobility. Therefore, we propose that growth of graphene proceeds rather differently, depending on the size and nature of the species that are being deposited. Specifically, we believe that one can design experiments such that either (i) adatoms are deposited onto the surface, or (ii) small clusters such as hexagons are the deposited species. The anticipated kinetics of these two modes of growths is rather different, as will be discussed in the following. It should be emphasized that the results presented here assume a pristine graphene surface while in practice graphene surfaces, especially the CVD grown graphene surfaces, are likely to suffer from inevitable contamination leading potentially to significantly impeded surface diffusion.

First, let us assume that the species used for deposition are single adatoms.[20] In that case, the adatoms are rather immobile, and the density of these adatoms increases essentially linearly with time. The formation of clusters begins only when the density of these adatoms becomes rather high and the probability of the collisions of multiple adatoms becomes significant during the growths. As the sizes of individual clusters grow, they become increasingly mobile. They become levitated when their sizes grow to at least 6 carbon atoms, and the mobility for surface diffusion reaches its peak. They will diffuse along the surface and incorporate the relatively immobile adatoms, while growing in size. With the increase of their sizes, they also slow down and eventually become as immobile as the adatoms.

When hexagons are deposited on the graphene surface,[21,22] these hexagons are very mobile, and essentially float on the surface. These hexagons collide and coalesce into larger graphene-like clusters and then slow down. Due to the large diffusion length of the hexagons, one could expect large area

and high quality graphene homoepitaxy with large grains at low growth temperatures. But we note that defects of grain boundaries may occur during coalescence for the following two reasons: (a) AA stacking and AB stacking are degenerate; (b) smaller building blocks such as monomers or dimers that are needed to fill in voids are absent.

These consequences need to be verified by carefully planned experimental studies. They also point to methods for optimizing the growths of precisely controlled bi-layer graphene. We propose to design experiments that use benzene as a source of diffusing species based on the fact that hexagons are very mobile. Other 2-dimensional van der Waals materials may follow similar growth mode as graphene which needs to be further verified.

Small carbon clusters are much more mobile than individual carbon adatoms on graphene surfaces. Due to the large diffusion length of carbon clusters, it is possible to conduct graphene epitaxial growth over graphene surfaces at low growth temperatures. Beyond a certain size of the cluster (24 atoms), a graphene-like structure is energetically preferred compared to a flat ring structure. Our results indicate that the growth mode of graphene homoepitaxy is totally different from the 3-dimensional bulk materials, and growth proceeds rather differently, depending on the size and nature of the species that are being deposited.

This work was supported in part by FAME, one of six centers of STARnet, a Semiconductor Research Corporation program sponsored by MARCO and DARPA. Y. H. Xie acknowledges the support from Alexander von Humboldt Foundation Research Award that made this research possible. The authors would like to thank Dr. Jakub Kaminski for his helpful suggestions.

[1]K. S. Novoselov, A. K. Geim, S. V. Morozov, D. Jiang, Y. Zhang, S. V. Dubonos, I. V. Grigorieva, and A. A. Firsov, Science **306**, 666 (2004).
[2]Y. Zhang, Y.-W. Tan, H. L. Stormer, and P. Kim, Nature **438**, 201 (2005).
[3]Y. M. Lin, C. Dimitrakopoulos, K. A. Jenkins, D. B. Farmer, H. Y. Chiu, A. Grill, and P. Avouris, Science **327**, 662 (2010).
[4]Y. Ji, S. Lee, B. Cho, S. Song, and T. Lee, ACS Nano **5**, 5995 (2011).
[5]Y. Yi, W. M. Choi, B. Son, J. W. Kim, and S. J. Kang, Carbon **49**, 4936 (2011).
[6]T. Cui, R. Lv, Z.-H. Huang, H. Zhu, Y. Jia, S. Chen, K. Wang, D. Wu, and F. Kang, Nanoscale Res. Lett. **7**, 453 (2012).
[7]Y. Sui and J. Appenzeller, Nano Lett. **9**, 2973 (2009).
[8]J. H. Deng, B. Yu, G. Z. Li, X. G. Hou, M. L. Zhao, D. J. Li, R. T. Zheng, and G. A. Cheng, Nanoscale **5**, 12388 (2013).
[9]R. J. Sun, Y. Zhang, K. Li, C. Hui, K. He, X. C. Ma, and F. Liu, Appl. Phys. Lett.**103**, 013106 (2013).
[10]K. M. F. Shahil and A. A. Balandin, Nano Lett. **12**, 861 (2012).
[11]M. Zhu, J. Wang, B. C. Holloway, R. A. Outlaw, X. Zhao, K. Hou, V. Shutthanandan, and D. Manos, Carbon **45**, 2229 (2007).
[12]T. Yu, C. Kim, and B. Yu, "Highly Conductive 3D Nano-Carbon: Stacked Multilayer Graphene System with Interlayer Decoupling," arXiv:1103.4567 (2011).
[13]V. Blum, R. Gehrke, F. Hanke, P. Havu, V. Havu, X. Ren, K. Reuter, and M. Scheffler, Comput. Phys. Commun. **180**, 2175 (2009).
[14]J. P. Perdew, K. Burke, and M. Ernzerhof, Phys. Rev. Lett. **77**, 3865 (1996).
[15]A. Tkatchenko and M. Scheffler, Phys. Rev. Lett. **102**, 073005 (2009).
[16]L. Xian and M. Y. Chou, J. Phys. D: Appl. Phys. **45**, 455309 (2012).
[17]K. W. Jacobsen, H. Jonsson, and G. Mills, "Nudged elastic band method for finding minimum energy paths of transitions," in *Classical and Quantum Dynamics in Condensed Phase Simulations*, edited by B. J. Berne, G. Ciccotti, and D. F. Coker (World Scientific, Singapore, 1998), p. 385.
[18]G. Henkelman and H. Jonsson, J. Chem. Phys. **113**, 9978 (2000).
[19]Q.-M. Zhang, C. Roland, P. Boguslawski, and J. Bernholc, Phys. Rev. Lett. **75**, 101 (1995).
[20]G. Lippert, J. Dabrowski, M. C. Lemme, C. M. Marcus, O. Seifarth, and G. Lupina, Phys. Status Solidi B **248**, 2619 (2011).
[21]G.-P. Dai, P. H. Cooke, and S. Deng, Chem. Phys. Lett. **531**, 193 (2012).
[22]Z. Li, P. Wu, C. Wang, X. Fan, W. Zhang, X. Zhai, C. Zeng, Z. Li, J. Yang, and J. Hou, ACS Nano **5**, 3385 (2011).